



Original article

Identification of anthranilamide derivatives as potential factor Xa inhibitors: Drug design, synthesis and biological evaluation



Junhao Xing^a, Lingyun Yang^a, Hui Li^a, Qing Li^a, Leilei Zhao^a, Xinning Wang^a, Yuan Zhang^b, Muxing Zhou^a, Jinpei Zhou^b, Huibin Zhang^{a, c, *}

^a Center of Drug Discovery, State Key Laboratory of Natural Medicines, China Pharmaceutical University, 24 Tongjiaxiang, Nanjing 210009, PR China

^b Department of Medicinal Chemistry, China Pharmaceutical University, Tongjiaxiang 24, 210009 Nanjing, PR China

^c Jiangsu Key Laboratory of Drug Discovery for Metabolic Disease, China Pharmaceutical University, Nanjing 210009, PR China

ARTICLE INFO

Article history:

Received 11 November 2014

Received in revised form

21 March 2015

Accepted 23 March 2015

Available online 25 March 2015

Keywords:

Factor Xa

FBDD

Structure-based pharmacophore

Consensus docking

Prothrombin time

Anticoagulant

ABSTRACT

The coagulation enzyme factor Xa (fXa) plays a crucial role in the blood coagulation cascade. In this study, three-dimensional fragment based drug design (FBDD) combined with structure-based pharmacophore (SBP) model and structural consensus docking were employed to identify novel fXa inhibitors. After a multi-stage virtual screening (VS) workflow, two hit compounds **3780** and **319** having persistent high performance were identified. Then, these two hit compounds and several analogs were synthesized and screened for in-vitro inhibition of fXa. The experimental data showed that most of the designed compounds displayed significant in vitro potency against fXa. Among them, compound **9b** displayed the greatest in vitro potency against fXa with the IC₅₀ value of 23 nM and excellent selectivity versus thrombin (IC₅₀ = 40 μM). Moreover, the prolongation of the prothrombin time (PT) was measured for compound **9b** to evaluate its in vitro anticoagulant activity. As a result, compound **9b** exhibited pronounced anticoagulant activity with the 2 × PT value of 8.7 μM.

© 2015 Elsevier Masson SAS. All rights reserved.

1. Introduction

Thromboembolic diseases are a leading cause of mortality worldwide [1,2]. The traditional pharmacotherapies to treat these diseases such as heparins and vitamin K antagonists have been proved to be effective in the prevention and treatment of these thrombotic disorders, but considerable therapeutic limitations (parenteral administration, numerous food and drug interactions, inconvenience of frequent monitoring, numerous drug and food interactions, etc.) restrict their clinical utilization [3], which prompts investigators to continue the search for novel oral anticoagulant not only possessing the same or higher therapeutic efficacy but also free of the disadvantages typical for the traditional medicines [4,5]. Factor Xa, which is situated at the juncture of intrinsic and extrinsic pathways in the coagulation cascade and catalyzes the conversion of prothrombin to thrombin, plays

prominent roles in various thromboembolic complications. It has been well demonstrated that the selective inhibition of fXa could provide an anticoagulant effect by blocking the amplified formation of thrombin without influencing normal hemostasis [6], which means that fXa inhibitors could decrease risk of bleeding. So many efforts have been devoted to search for novel fXa inhibitors with a favorable safety profile [7–9]. Currently, three oral, direct, selective factor Xa inhibitors have been approved: rivaroxaban [10–12] (Bayer), apixaban [13,14] (Bristol-Myers Squibb/Pfizer) and edoxaban (Daiichi-Sankyo) [15,16] by the U.S. Food and Drug Administration (FDA) (Fig. 1). Several other promising fXa inhibitors, such as brixaban and eribaxaban, are currently under various stages of clinical trials [17–20].

FBDD, which adopts an effective strategy that increased activity is obtained by integrating several independent functional fragments with low-affinity binding together, is a promising paradigm in lead discovery [21–24]. The preference for FBDD over other methods, such as high throughput screening (HTS), rests largely on the enhanced screening of a more impressive conformational space with a smaller starting number of compounds [25,26]. On the other hand, the methodology has earned great reputation in rapidly discovering potential drug leads at relatively lower cost of

* Corresponding author. Center of Drug Discovery, State Key Laboratory of Natural Medicines, China Pharmaceutical University, 24 Tongjiaxiang, Nanjing 210009, China.

E-mail addresses: xingjhcpu@163.com (J. Xing), hb_zhang@hotmail.com (H. Zhang).

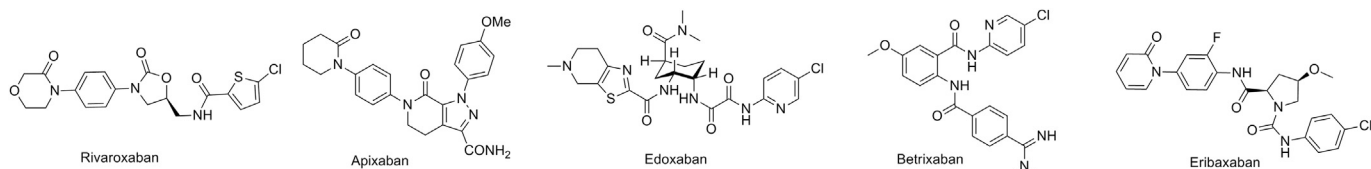


Fig. 1. The structures of rivaroxaban, Apixaban, Edoxaban, Betrixaban and Eribaxaban.

economic investment than biophysical approaches such as nuclear magnetic resonance (NMR), X-ray diffraction, surface plasmon resonance (SPR) and mass spectrometry (MS) [27]. Therefore, in our study, the strategy for three-dimensional fragment-based lead discovery [26] was employed to discover novel compounds with fXa inhibitory potency. Specifically, some known structurally diverse fXa inhibitors with co-crystallized conformations were firstly overlaid and then deconstructed into small groups according to the predefined rules. The resulted fragments that occupy different regions of the active site were then merged or linked to generate the novel, potential fXa inhibitors. Several screening technologies, such as structure-based key pharmacophore constraints, consensus docking screening and ADMET, were carried out to screen the new molecular library generated through chemical space analysis to identify the potential active molecules. The root-mean square deviation (RMSD) values between the docking and combining conformations of the new compounds were calculated and chosen as the main standards for lead identification. The flowchart of each procedure was shown in Fig. 2. Finally, two hit

compounds combined with several analogs were synthesized and subsequently evaluated for their inhibitory activity against fXa, and the compound showing the most potent activity of fXa inhibition was further assessed the degree of selectivity versus thrombin and extension of the prothrombin time (PT). The results obtained from FBDD and biological experiment would provide noteworthy information for further development of fXa inhibitors.

2. Results and discussion

2.1. Fragment library

There were approximately 114 fXa-inhibitor cocrystal structures [28–34] available in the protein data bank (PDB) when this article was prepared. Thirty-nine representative fXa inhibitors were selected based on the diverse structures of the co-crystallized ligands (Fig. 3) and then overlaid with the reference structure. Therefore, the active conformations of the ligands were also well overlaid within the same coordinate system. The generated



Fig. 2. The flowchart of the novel hits discovery strategy.

fragment library was comprised with 305 fragments based on the 39 known ligands under the established setting rules. The information about the spatial distribution in the target was included in the resultant fragment library, as well as about their chemical structures. The binding conformations of inhibitor rivaroxaban (PDB code 2w26) and its fragments were shown in Fig. 4, and it was found that the inhibitor was deconstructed into three component fragments which maintained the initial orientations and spatial positions of the ligand.

2.2. Evaluation of fragment-based compound library and hits identification

2.2.1. Construction of new molecular library

According to the setting rules, All the new molecules should be constructed by the fragments from different initial sets (Fig. 5). As a result, 11858 compounds were developed from 305 fragments by chemical space analysis.

2.2.2. Lipinski's rule and ADMET profile

To effectively abandon the redundant compounds and generate a library with high quality, some virtual screening, including Lipinski's rule and ADMET profile, was firstly performed to filter the new molecules. Finally, 814 compounds were selected from the library.

2.2.3. Structural based pharmacophore generation

Twelve fXa-inhibitor cocrystal structures which were included in the above mentioned thirty-nine representative fXa inhibitors were superimposed with the same coordinate. The Ludi interaction map was used to generate pharmacophore features which consisted of hydrogen bond acceptor (HBA), hydrogen bond donor (HBD), aromatic ring and hydrophobic features (Fig. 6A and B). Then some common pharmacophoric constraints in the active site of fXa were retained and some unrepresentative features were deleted. As a result, six sets were considered as the key pharmacophoric features (Fig. 6C). Subsequently, the central pharmacophore feature of each set was defined as the common feature and constructed the Hypo1 (Fig. 6D). Hypo1 was then aligned to rivaroxaban. As were shown in Fig. 6E and F, one HBA and HBD, one aromatic ring in the S4 pocket, two hydrophobic cores in S1 pocket, one HBA and one HBD were all included in the SBP model. Eventually, Hypo 1 was employed as the query to quickly identify compounds in the library generated from last stage, which have an excellent mapping. As a result, 380 compounds were well matched this model.

2.2.4. Consensus docking

The compounds resulting pharmacophore screening were then analyzed by docking study. Presently, there are many potential pitfalls and inherent limitations remaining in docking program. There is no single docking program that is competent in all cases, which poses a pressing question regarding the optimal protocol to select for docking-based virtual screening. Recent studies have reported a novel consensus docking strategy, which instead of combining various docking scores, comprehensively integrated the results of docking poses from separate docking programs [35–37]. The use of consensus docking poses could remarkably improve the reliability of docking and remedy the drawback existing in single docking program, which always provide similar docking scores with no way of distinguishing which one is correct [36]. Previously, we have successfully adopted this method in identification of dipeptidyl peptidase IV inhibitors [37]. Now, consensus docking strategy is also employed by using the following two different docking programs: LigandFit in DS2.5 and glide in Schrodinger 2009. DockScore and GScore were selected to separately rank

docked poses in each program. During screening, the recommended criterion for similar docking results was slightly modified from $\text{RMSD} < 2.0 \text{ \AA}$ to $\text{RMSD} < 3.0 \text{ \AA}$ because of limited number of hit compounds when the proposed criteria applied. The 380 top-ranking hit compounds from last step were independently docked to the fXa structure (PDB code 2w26) by LigandFit and Glide. And the top 100 compounds resulting from each docking program were combined, and their poses were compared visually followed by the calculation of corresponding RMSD value (RMSD_1 in Fig. 7). As a result, 43 compounds containing similar docked poses generated from two different docking programs were considered to be valid docking results.

2.2.5. RMSD-based scoring function

To further evaluate the quality of the 43 compounds, the RMSD values between the combining conformations and the predicted binding conformations which were generated from molecular docking were then calculated to re-rank hit compounds. The RMSD values of the 43 compounds were showed in Fig. 7 (RMSD_2), and it was found that most of them were distributed around 2.00 Å, with five compounds $< 1.00 \text{ \AA}$ and three $> 3.00 \text{ \AA}$. Table 1 exhibits all the detailed RMSD values of the 43 potential fXa inhibitors in ascending order, and Table 2 lists the structures of top-ten new compounds generated by this stage. Among them, three known compounds (1876, $\text{RMSD} = 0.1487$, $\text{K}_i = 0.14 \text{ nM}$; 2398, $\text{RMSD} = 0.3021$, $\text{IC}_{50} = 27 \text{ nM}$; 643, $\text{RMSD} = 1.1324$, $\text{K}_i = 90 \text{ nM}$) with good fXa inhibitory activity were also constructed with the fragments from the different initial inhibitors. From the comparison of RMSD values and activity data of the three compounds, we can find that the smaller deviations between their binding and combining conformations that they obtain, the higher inhibitory activity they will display. This correlation is consistent with our assumption. The RMSD values of top-ten new compounds were all small and in the range from 0.1487 to 1.3938, indicating that all fragments maintained their original conformation and binding mode in the newly constructed molecules which would show good activity against fXa with a high probability. As for the selection of hits compounds, synthetic tractability and cost were firstly considered. As a result, compounds **3780** and **319** were chosen as hit compounds.

The interaction mode of two hit compounds with fXa predicted by glide in Schrodinger 2009 were illustrated in Fig. 8. For the interaction mechanism of **3780** with fXa (Fig. 8a), 5-chlorothiophene occupies hydrophobic S1pocket formed by Ala190, Val213 and Tyr228 and forms a $\text{Cl}-\pi$ interaction between the chloro atom and the phenyl ring of Tyr228, which played a part in the interaction between inhibitors and fXa. The NH of scaffold carboxamide forms a hydrogen bond with carbonyl oxygen of Gly219. The P4 phenyllactam of **3780** is flanked by the phenyl groups of Phe174 and Tyr99 in the S4 aryl binding pocket and forms an edge to face interaction with Trp215. The carbonyl oxygen (scaffold carboxamide) also forms hydrogen bond with Gly216. For Compound **319** (Fig. 8B), chloropyridine occupies the S1 pocket more deeply than **3780** because the carboxamide group extends P1 by 2-bonds length, but $\text{Cl}-\pi$ interaction with Tyr228 was not formed because the chlorine atom deviated from the phenyl ring of Tyr228. The other interaction mode is similar to **3780**.

To confirm the reliability of the strategy, compounds **3780** and **319** were firstly synthesized and evaluated for in vitro inhibition of fXa. To our delight, the two compounds exhibited inhibitory activity against fXa with the IC_{50} value of 67 nM and 298 nM, respectively, which encouraged us to further explore the efficacy of analogs of these two hit compounds. As a result, a series of analogs of compounds **3780** and **319** were designed, synthesized and evaluated for their fXa inhibitory activity.

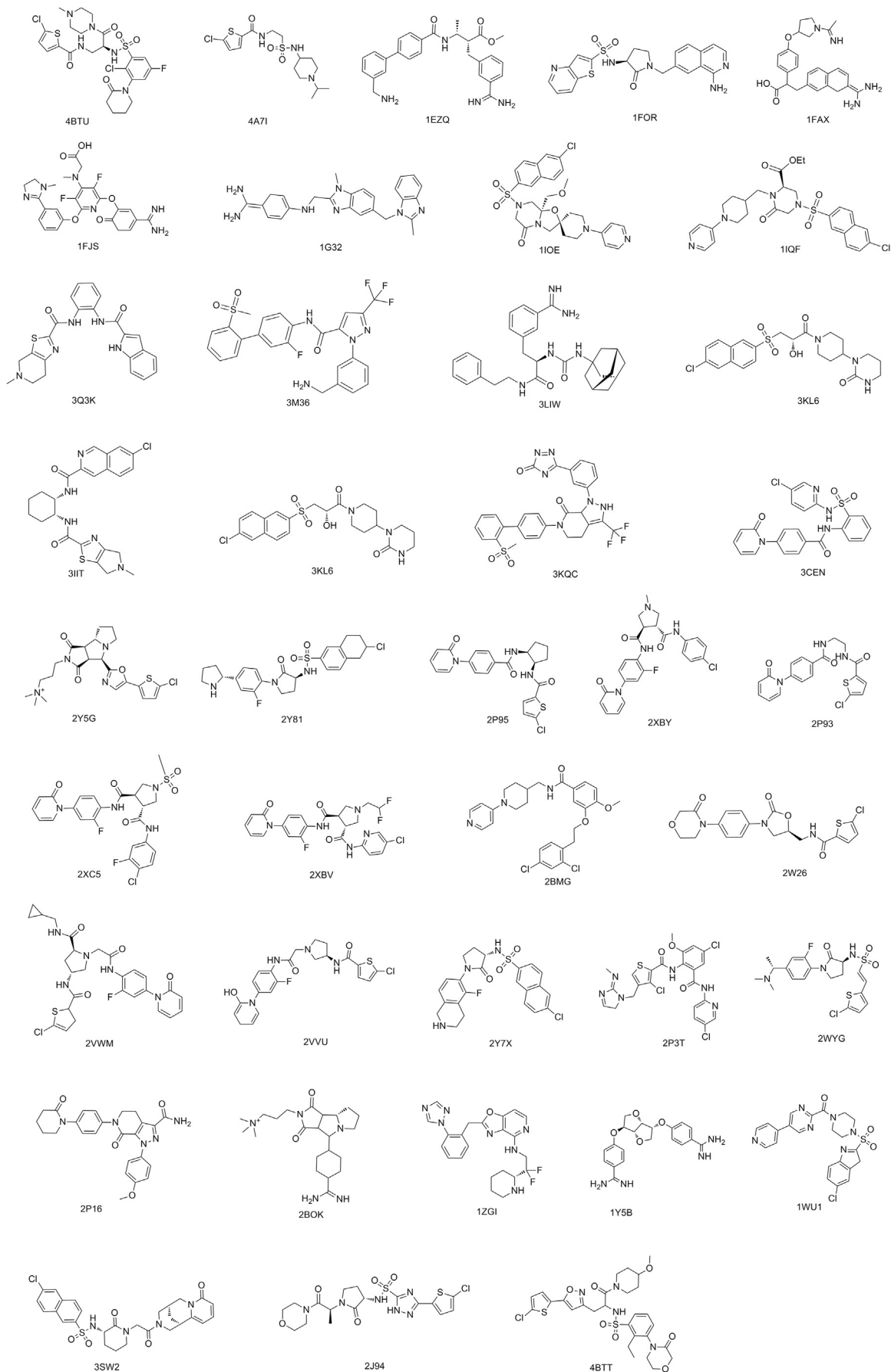


Fig. 3. Chemical structures of initial 39 known inhibitors that were cocrystallized with fxa.

2.3. Chemistry

The synthetic routes of intermediates and target compounds **9a–e** and **12a–g** are depicted in Scheme 1. The commercially starting material available **1** was treated with chloroacetyl chloride to generate compound **2** [38], which was further converted to intermediate **4** ($X = O$) through treating with nitric acid in concentrated sulfuric acid at 0 °C [39]. Additionally, treatment of the commercially available **3** with 5-chlorovaleryl chloride using excess sodium hydroxide afforded **4** ($X = CH_2$). Hydrogenation of **4** using Pd/C (10%) and hydrazine hydrate (80%) in anhydrous EtOH provided aniline **5**, which was acylated by **6** to afford **7**. Nitro-reduction of **7**, followed by acylation with aromatic acid afforded corresponding target compounds **9a–e**. Alternatively, treatment of compound **8** ($X = O$) with ethyl oxalylmonochloride provided oxoacetate analog **10**. Hydrolysis (KOH (1 N) in THF/water) of **10** gave oxoacetic acid intermediate **11**, which was subsequently converted to compounds **12a–g** by acylation with aromatic amines.

The physical characteristics, IR, 1H NMR, ^{13}C NMR, MS and elemental analysis data for all intermediates and target compounds, were reported in the supporting information.

2.4. Biological activities and discussion

2.4.1. In vitro inhibition activities studies of fXa

All the targeted compounds were evaluated in vitro for their fXa enzyme inhibitory activity, and betrixaban has been selected as the positive control. Tables 3 and 4 summarized the fXa inhibitory activity of designed compounds. The assay results showed that most of the novel compounds exhibited significant inhibitory activity against fXa with the IC_{50} value from 1120 to 23 nM (Table 4), particularly for compound **9b**, which was the most potent fXa inhibitor in these series with the IC_{50} value of 23 nM.

The experimental data showed that the compound **12a**, which was non-substituted at the benzene ring, showed weak fXa inhibition activity with the IC_{50} value of 1120 nM. The mono-chloro substituted compounds demonstrated regiochemical preferences of para > meta > ortho (**12b** = 798 nM, **12c** = 621 nM, and **12d** = 452 nM). Of the synthesized compounds **12a–g**, a chlorine group (**12d**) at the paraposition exhibited most potent compound of this series. An activity difference between chloro- and fluoro-substitution was also found in this series. 4-fluoro substituent analog **12e**, which was more active than non-substituted **12a**, was 1.5-fold less potent in the binding assay compared with the 4-chloro substituted compound **12d**. Additionally, methoxyphenyl analogs **12f**, **12g** were also more active than **12a**, and an activity order of para > ortho was also observed. Replacement of oxalamide group in **12a–g** with amide group increased activity dramatically (**12a–g** vs **9a–e**). In a similar trend to that observed in **12a–g**, the unsubstituted phenyl analog **9a** exhibited moderate fXa inhibitory activity with the IC_{50} value of 512 nM. Chlorophenyl analogs **9c** and **9d** were more potent than **9a**, and **9b** (4-Cl) exhibited the most potent fXa inhibition in vitro with the IC_{50} of 23 nM. Introduction of methoxy group at para or meta-position could slightly improve fXa inhibitory activity and an activity order of para > meta was observed (**9d** = 286 nM, **9e** = 378 nM).

2.4.2. Selectivity versus thrombin and prothrombin time (PT) assay

In view of its excellent bioactivity in the primary fXa assay, **9b** was chosen to assess the degree of selectivity versus thrombin and the extension of the prothrombin time (PT) to determine its in vitro anticoagulant activity. The assay results were showed in Table 5, which demonstrated that **9b** not only exhibited weak activity against thrombin with an IC_{50} value of 48 μ M but also showed excellent in vitro anticoagulant activity, judging by its $2 \times$ PT value

of 8.7 μ M. Although compound **9b** was less active than betrixaban in the fXa binding assay, it showed similar selectivity against thrombin and a comparable magnitude in anticoagulant activity in vitro with betrixaban.

3. Conclusion

In summary, we have reported a drug design strategy which integrated FBDD, structure-based key pharmacophore and structural consensus docking for identification of novel fXa inhibitors. Then two hit compounds together with their analogs were synthesized and evaluated for potential inhibitory activity against fXa. In vitro evaluation demonstrated that most of test compounds displayed evident fXa inhibition. Of these derivatives, compound **9b** was found to possess the best fXa inhibitory activity with an IC_{50} value of 23 nM and excellent selectivity over thrombin (48 μ M). In vitro anticoagulant activity, compound **9b** also exhibited pronounced anticoagulant activity with the $2 \times$ PT value of 8.7 μ M. Therefore it could be considered as lead compound for obtaining even more potent fXa inhibitors and may be eventually developed into new anticoagulant drugs candidates against fXa.

4. Experimental section

4.1. fXa inhibitors set collection

All the compounds were selected according to the following rules: (i) Compounds should bind to the same active site of fXa; (ii) The known inhibitors selected should cover diverse chemical structures. Most fXa inhibitors collected could be found their crystal complex structures in PDB. Without the experimentally resolved structures of the inhibitors within the complex of the target protein, accurate molecular docking simulations were employed to generate their binding conformations. All the compounds were well-aligned the reference crystal structure keeping the original technical parameter of the protein structural alignment software default, and then their binding conformations were extracted from the complex structures to generate three-dimensional fragments [26].

4.2. Three-dimensional fragment generation

The corresponding fragment located in different regions of the target were generated by deconstructing the superimposed compounds with their binding conformations according to some simple rules, similar to those described in the original report on the retrosynthetic combinatorial analysis procedure (RECAP) [40]. According to this principle, ring connecting bonds and hydrogen bonds should not be cut, and molecules with more than the defined "maximum atoms" (i.e., maximum number of atoms allowed in the compound to be cleaved) were not cut. The minimum number of non-hydrogen atoms in a fragment was set to 2. It was an option to set whether the bonds between heteroatoms and carbons are allowed to cleave. The resultant fragments were denominated in the same way described in previously reported literature [26]. All generated fragments in the library were not only well matched with separate regions in the target, but also maintained their original conformations and binding modes of the selected inhibitors with fXa.

4.3. Construction of new molecules

The construction of new compounds was implemented automatically through linking or merging the neighboring three-dimensional fragments through a series of bonding rules

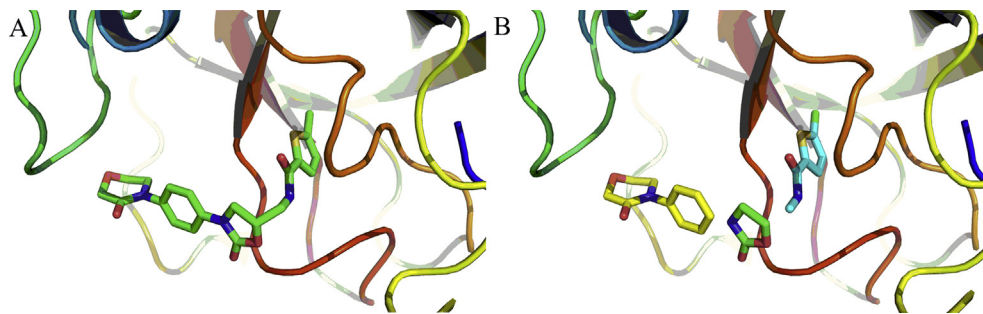


Fig. 4. (A): Binding conformation of rivaroxaban (PDB code 2w26). (B) Conformations of the three constituted fragments deconstructed from rivaroxaban: fragment 1 (yellow), fragment 2 (green), and fragment 3 (cyan). (For interpretation of the references to colour in this figure legend, the reader is referred to the web version of this article.)

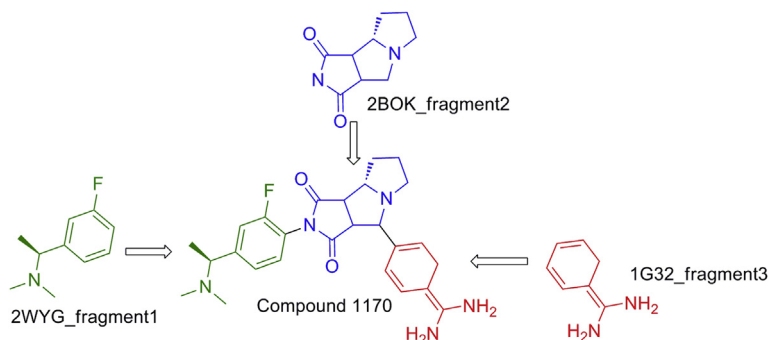


Fig. 5. Compound 1170, a potential inhibitor of fXa, constructed from fragments of three different known inhibitors.

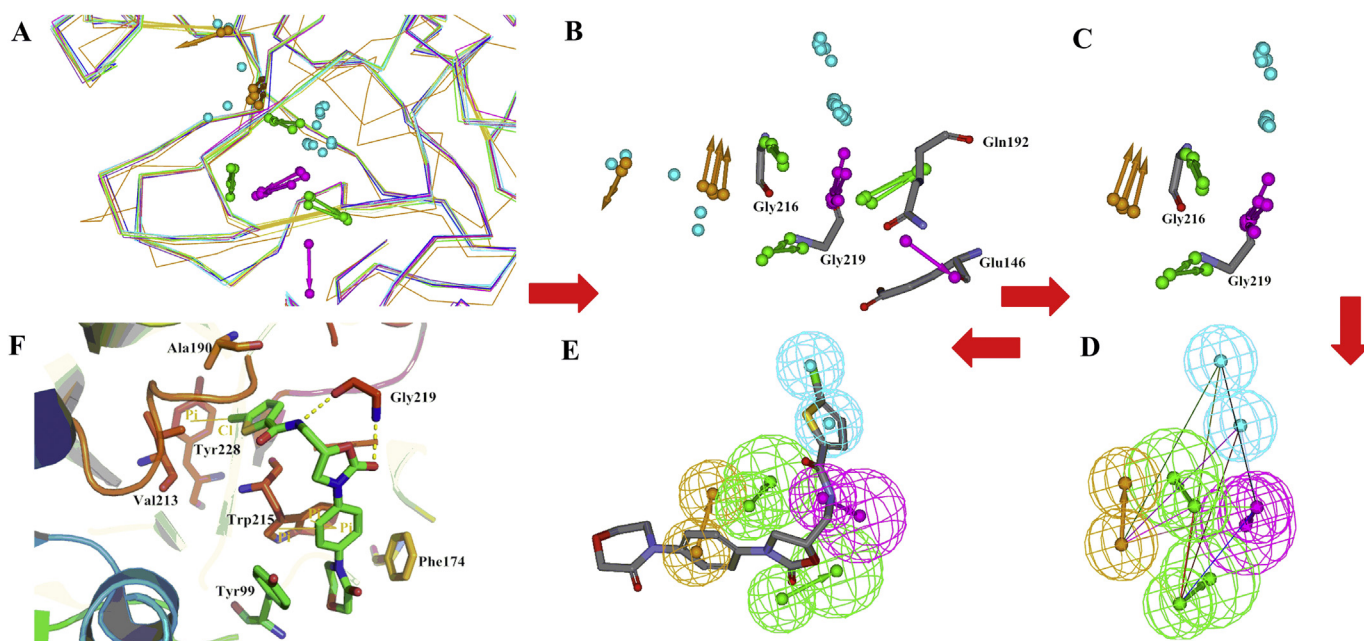


Fig. 6. (A) All 12 pharmacophore queries aligned to define the common features. (B) The pharmacophoric constraints in the active site of fXa. (C) The key features were retained according to the clustering rule; (D) The SBP model consisted of common features; (E) Best pharmacophore model Hypo1 aligned to rivaroxaban; (F) Interactions of rivaroxaban with the active site of fXa (PDB code 2w26).

described in the literature [26]. The bonds which could be formed between the fragments have been firstly identified by the following criteria: (a) the angle between the bond directions should be less than 15° , and (b) the distance between the atom that remains in one fragment and the atom that leaves the other fragment should

be less than a threshold 1 \AA . The first rule guarantees the adequate rotational alignment of the generated fragments, and the second criterion ensures the proper translational alignment of the fragments. Both internal and peripheral bonds could be considered for disconnection to form a new bond with another fragment, and the

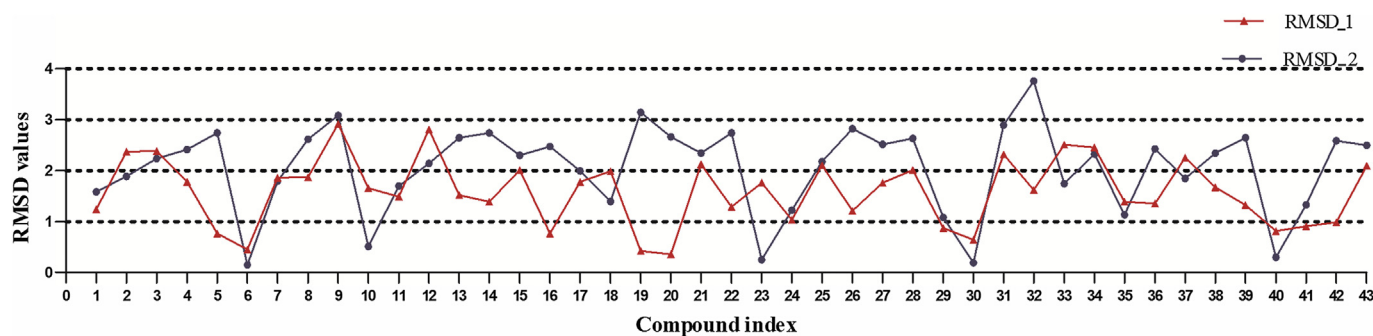


Fig. 7. RMSD value distribution of the 43 potential fXa inhibitors.

Table 1
Ranking of the 43 potentially fXa inhibitors using the RMSD values.

Index	Compound name	RMSD ^a	RMSD ^b	Ranking	Index	Compound name	RMSD ^a	RMSD ^b	Ranking
6	1876	0.4525	0.1487	1	21	254	2.1234	2.3436	23
30	8769	0.6459	0.1921	2	38	4913	1.6723	2.3449	24
23	432	1.7625	0.2539	3	4	470	1.7825	2.4137	25
40	2398	0.8172	0.3021	4	36	532	1.3526	2.4286	26
10	752	1.6580	0.5124	5	16	6841	0.7652	2.4762	27
29	3780	0.8762	1.0841	6	43	791	2.0941	2.4987	28
35	643	1.3897	1.1324	7	27	4592	1.7624	2.5132	29
24	1771	1.0346	1.2234	8	42	35	0.9851	2.5856	30
41	7425	0.9071	1.3324	9	8	609	1.8724	2.6142	31
18	319	1.9872	1.3938	10	28	7812	2.0116	2.6354	32
1	853	1.2398	1.5823	11	39	10061	1.3240	2.6437	33
11	4612	1.4891	1.6984	12	13	211	1.5217	2.6483	34
33	6783	2.5091	1.7425	13	20	890	0.3561	2.6637	35
7	289	1.8616	1.7942	14	5	9217	0.7653	2.7381	36
37	1082	2.2546	1.8482	15	22	8203	1.2901	2.7420	37
2	3147	2.3712	1.8887	16	14	335	1.3924	2.7414	38
17	10342	1.7832	1.9912	17	26	168	1.2093	2.8216	39
12	2651	2.8109	2.1432	18	31	3245	2.3218	2.8937	40
25	726	2.1092	2.1789	19	9	5872	2.9174	3.0824	41
3	3128	2.3876	2.2341	20	19	901	0.4238	3.1417	42
15	122	2.0136	2.3014	21	32	861	1.6218	3.7276	43
34	913	2.4580	2.3237	22					

^a The RMSD values were calculated between the docking poses generated from LigandFit and Glide.

^b The RMSD values were calculated between the combining conformations and the predicted binding conformations.

fragments could overlap. However, if the distance between the fragment centroids was below the refined threshold of 3.0 Å, then the fragments could not join because they were considered to occupy the same location in the receptor. The self-assembly of fragments was performed after four steps. The first step connects pairs of fragments. In the second step, the results of the first procedure were used as input, so that the generated compounds can be the combinations of up to four fragments, and so on. Four rounds were carried out so that the new compounds could be generated by the constituent molecules from the previous step. The new molecules should not be constructed with the fragments from the same inhibitor to guarantee the novelty of the generated compounds, judging from the fragment denomination. For fragments that contained no atoms which were close enough to generated new bonds, methylene linkers (at most two) were added to combine the adjacent fragments and formed a single drug-like compound. Additionally, fragment merging was performed if the carbon–hydrogen or carbon-halogen bonds in the different fragments bound in proximal regions overlapped. Generally, a total molecule obtained by combining adjacent fragments was handled by energy minimization. However, all the new compounds were not subjected to the energy minimization procedure in this strategy, so that the constituent fragments of the constructed compounds would keep their original conformations in the protein-binding pocket.

4.4. Evaluation of constructed molecular library

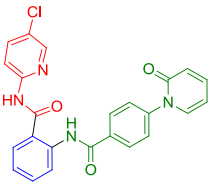
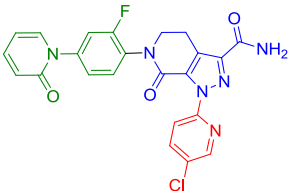
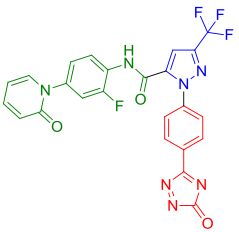
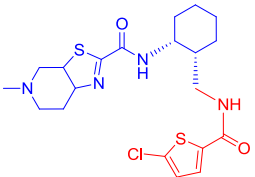
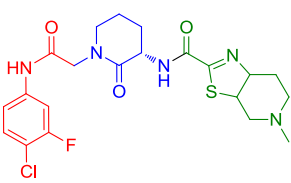
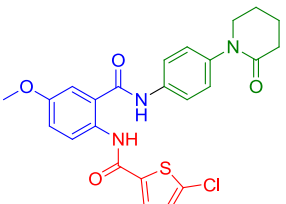
4.4.1. In silico evaluation of the Lipinski's rule and ADMET profile

The Lipinski's rule of five parameters—molecular weight (MW), AlogP, number of hydrogen bond donors (HBD), number of hydrogen bond acceptors (HBA), and molecular fractional polar surface area were firstly employed to qualitatively estimated their potential “drug-like” properties. ADMET descriptors can be added if other criteria are required. The generated molecular library is subjected to this filtration through employing the Calculate Molecular Properties protocol available in discovery studio 3.0, and all the parameters in the Parameters Explorer were in default.

4.4.2. Structure-based key pharmacophore generation

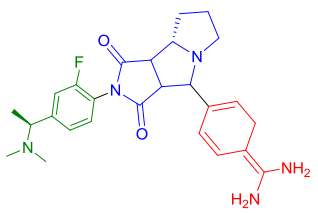
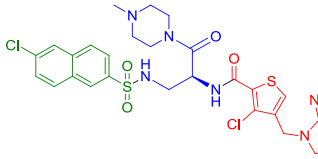
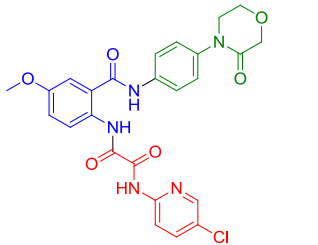
Structure-based key pharmacophore models were generated based on 12 complex structures (4BTI, 3Q3K, 3M36, 3LIW, 3KQC, 3IIT, 2Y81, 2Y5G, 2P16, 2W26, 1WU1 and 1G32) with a Ludi interaction map using receptor-ligand pharmacophore generation protocol with default parameters in DS3.0. This protocol created a pharmacophore query from a Ludi interaction map which was created in a receptor active site sphere and consists of hydrogen bond acceptor, hydrogen bond donor, and hydrophobic features. Finally 12 pharmacophore models were generated, which were then aligned and reserved the most common features to generate a

Table 2
The structures of top-ten new compounds generated by this stage.

Compound name	Structures	RMSD ^a	Fragment 1 (blue)	Fragment 2 (green)	Fragment 3 (red)	IC ₅₀ /Ki(nM)
1876		0.1487	3Q3K_ fragment2	2P95_ fragment3	2XBV_ fragment4	Ki = 0.14
8769		0.1921	2p16_ fragment1	2XBV_ fragment1	2XBV_ fragment3	—
432		0.2539	3M36_ fragment1	2XC5_ fragment5	3KQC_ fragment3	—
2398		0.3021	3IIT_ fragment5		2W26_ fragment3	IC ₅₀ = 27
752		0.5124	3SW2_ fragment2	3Q3K_ fragment3	2XC5_ fragment5	—
3780		1.0841	Berixaban_ fragment1	2p16_ fragment3	2w26_ fragment3	—
643		1.1324	2J94_ fragment1		1WU1_ fragment4	Ki = 90

(continued on next page)

Table 2 (continued)

Compound name	Structures	RMSD ^a	Fragment 1 (blue)	Fragment 2 (green)	Fragment 3 (red)	IC ₅₀ /Ki(nM)
1771		1.2234	2BOK_ fragment2	2WYG_ fragment1	1G32_ fragment3	—
7425		1.3324	4BTU_ fragment2	11OE_ fragment1	2P3T_ fragment6	—
319		1.3938	Berixaban_ fragment1	Edoxaban_ fragment 2	2p16_ fragment2	—

^a The RMSD values were calculated between the combining conformations and the predicted binding conformations.

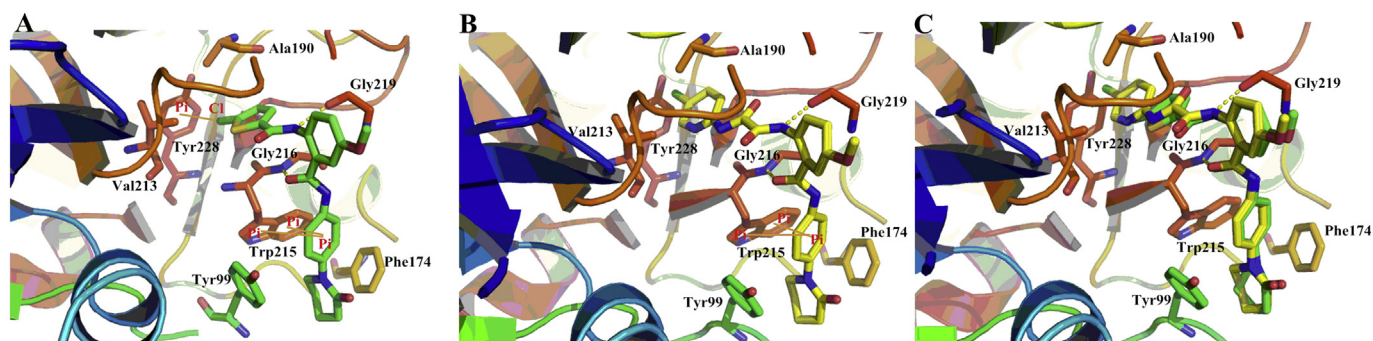


Fig. 8. The docking model of compounds **3780** and **319** with the binding site of fXa. (A): The interactions of compound **3780** with the active site of fXa. (B): The interactions of compound **319** with the active site of fXa. (C): Overlay of binding conformations of compounds **3780** and **319** with the active site of fXa. Hydrogen atoms have been hidden for clarity. The figures were prepared using PyMol (www.pymol.org).

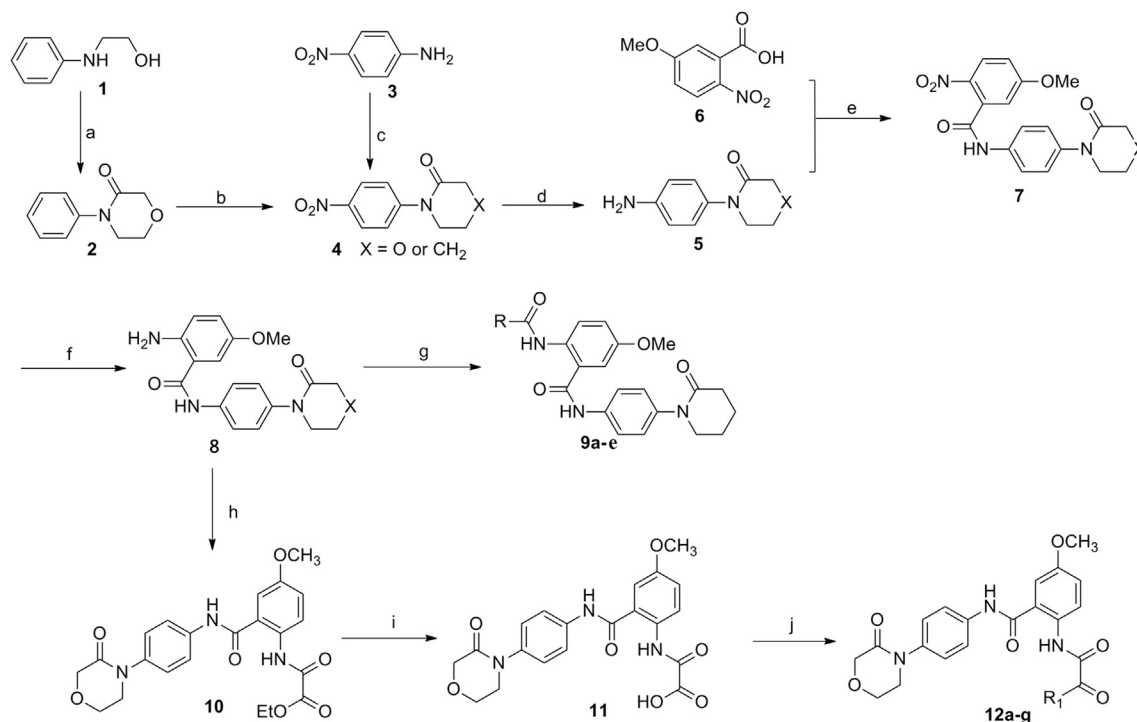
SBP model, Hypothesis 1 (Hypo 1). Subsequently, Hypo 1 was employed to filter the new molecular library obtained by last strategy.

4.4.3. Docking simulation

All the molecules, which passed ADMET and the pharmacophore screening, were prepared using the LigPrep module in Schrodinger 2009 and two parallel docking studies were independently conducted employing LigandFit available in DS2.5 and Glide in Schrodinger 2009 to determine a consensus docked pose for each molecule, as described in our previous study [37], and fXa structure used as receptor in docking was retrieved from the protein data bank (PDB entry: 2w26) [32]. For each molecule, the RMSD value was calculated between the docked poses from Glide and Ligandfit. This value gives us a direct measurement to assess the accuracy of docking results. When the RMSD value between two docking results is larger than 3 Å, there is a high probability to be false positive hit.

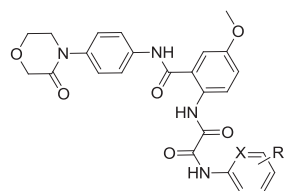
4.4.4. Hit selection

The generated combining conformations of the novel compounds maintained the original binding modes of their constituent fragments because the energy minimization procedure was not applied in this strategy. Glide in Schrodinger 2009 was employed to simulate the binding conformations of the new compounds with fXa. To confirm whether the constituent fragments in the generated molecules maintained their original binding modes, the RMSD value between the combining and docking conformations is used as a criterion to assess the conformational distortions of the component fragments. The lower RMSD values molecules obtain, the higher potential activity they will display. When the RMSD value between the combining and docking conformations below 3 Å, it suggests that the fragments are combined without remarkable distortions of their individual binding modes in the final molecules. The combining and docking conformations are imported into molecule window in DS3.0. Calculate Docked Rmsd calculates the RMSD of atoms in the combining conformation with respect to docking conformation. The RMSD values are calculated between



Scheme 1. Synthesis routes and structures of intermediates and target compounds. Reagents and conditions: (a) Chloroacetyl chloride, EtOH/H₂O, NaOH, 38–45 °C, 1 h; (b) sulfuric acid; nitric acid –10 °C, 1 h; (c) 5-Chlorovaleryl chloride, NaOH, THF/H₂O, 0-rt, overnight; (d) hydrazine hydrate (80%), Pd/C (10%), EtOH, reflux, 1 h; (e) Oxalyl chloride, DMF, CH₂Cl₂, 0-rt, 1 h, then CH₂Cl₂, triethylamine, 0-rt, 16 h; (f) hydrazine hydrate (80%), Pd/C (10%), EtOH, reflux, 1.5 h; (g) aromatic carboxylic acid, Oxalyl chloride, DMF, CH₂Cl₂, 0-rt, 1 h, then CH₂Cl₂, triethylamine, 0-rt, 14 h; (h) ethyl oxalylmonochloride, CH₂Cl₂, N,N-Diisopropylethylamine, 0-rt, 1 h; (i) KOH, H₂O/THF, Hydrochloric acid (1 N), 1 h, 0-rt; (j) EDCI, DMAP, aromatic amines, DMF, rt, 120 h.

Table 3
fXa inhibitory effect of designed compounds **319** and **12a–g**.



Compound	X	R	IC ₅₀ (nM) ^a
319	N	5-chloro	298
12a	CH	H	1120 ± 145
12b	CH	2-chloro	798 ± 92
12c	CH	3-chloro	621 ± 67
12d	CH	4-chloro	452 ± 46
12e	CH	4-fluorine	678 ± 72
12f	CH	2-methoxy	828 ± 101
12g	CH	4-methoxy	612 ± 59

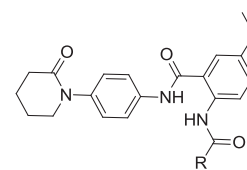
^a The data represent the mean of at least three independent determinations.

two conformations, including hydrogen atoms.

4.5. Chemistry

All starting materials, solvents and reagents were commercial sources and used without further purification. All the reactions mentioned in this article were monitored by thin layer chromatography (TLC) at 254 nm under a UV lamp with the following eluent system: n-hexane/ethyl acetate or dichloromethane/methanol. Column chromatography separations were obtained on silica gel (300–400 mesh) eluting with CH₂Cl₂/MeOH (60/1). %Purity of the target compounds (>97%) were determined by HPLC analysis

Table 4
fXa inhibitory effect of designed compounds **3780** and **9a–e**.



Compound	R	IC ₅₀ (nM) ^a
3780		67 ± 18
9a		521 ± 59
9b		23 ± 8
9c		183 ± 22
9d		286 ± 34
9e		378 ± 49

^a The data represent the mean of at least three independent determinations.

(UV detector, wavelength: 230 nm). ¹H NMR and ¹³C NMR spectra on a Bruker AV 300 MHz spectrometer were recorded in DMSO-*d*₆ or CDCl₃. Chemical shifts are recorded in δ (ppm) units relative to

Table 5
Selectivity versus thrombin and anticoagulant activity of **9b**.

Compound	Thrombin IC ₅₀ (μM) ^a	2 × PT (μM) ^b
9b	48	8.7
Betrixaban	18	2.4

^a The data represent the mean of at least three independent determinations.
^b 2 × PT value is defined as the inhibitor concentration required to double the time to fibrin formation.

TMS. Mass spectrometry (MS): Hewlett–Packard 1100 LC/MSD spectrometer, in *m/z*; Elemental analyses: CHN–O–Rapid instrument.

4.6. Inhibition of fXa and thrombin *in vitro*

The synthesized compounds were measured *in vitro* for their factor Xa/thrombin inhibition using achromogenic substrates. The targeted compounds were prepared at 10 mM concentration and then serially diluted to give twelve different aliquots spanning a range of 0.010–500 μM in buffer (50 mM Tris–Cl, 100 mM NaCl, 0.1% BSA, pH 7.4). The final enzyme concentrations were 0.003 U/mL (human fXa from Enzyme Research Laboratories) and 0.125 U/mL (human thrombin from Sigma Chemical Co.). The reagents containing compound dilutions, buffer and enzyme were mixed, centrifuged, and incubated for 30 min at 37 °C in 96-well microtiter plates. The enzyme reaction was initiated by adding appropriate substrate (for factor Xa, S-2222; for thrombin, S-2238). The time course of the reaction was monitored continuously for 20 min at 405 nm in a microtiter plate reader. The IC₅₀ was calculated from the mean of duplicates from a dilution series of the compound with graphpad prism 5.

4.7. Prothrombin time (PT) assay

Commercially available kits (ThrombopLastin-DS from Fisher Diagnostics, a division of Fisher Scientific, Co.L.L.C.) were employed to measure PT. Clotting times were measured using an automatic coagulometer (BE Compact-X), in accordance with the manufacturer's instructions. Increasing concentrations of inhibitor or solvent were added to plasma and incubated for 3 min at 37 °C. The plasma clotting times were calculated and compared with those from the appropriate control plasma.

Acknowledgment

This study was supported by the Natural Science Foundation of Jiangsu Province (No. BK 20141349) and the China National Key Hi-Tech Innovation Project for the R&D of Novel Drugs (No. 2013ZX09301303-002).

Appendix A. Supplementary data

Supplementary data related to this article can be found at <http://dx.doi.org/10.1016/j.ejmech.2015.03.052>.

References

- [1] R. Carrillo-Esper, E. Alcantar-Luna, M.A. Herrera-Cornejo, D. Jaimovich, M.A. Ramos-Corralles, A. Villagomez-Ortiz, Practice guidelines for the implementation of a quality program in thromboprophylaxis and treatment management in patients with venous thromboembolic disease, *Cir. Cir.* 80 (2012) pp.92–105.
- [2] K.L. Furie, S.E. Kasner, R.J. Adams, G.W. Albers, R.L. Bush, S.C. Fagan, J.L. Halperin, S.C. Johnston, I. Katzan, W.N. Kernan, P.H. Mitchell, B. Oviabagele, Y.Y. Palesch, R.L. Sacco, L.H. Schwamm, S. Wassertheil-Smolter, T.N. Turan, D. Wentworth, C.o.C.N.C. o.C.C., American Heart Association Stroke Council, C.

- Interdisciplinary Council on Quality of, R. Outcomes, Guidelines for the prevention of stroke in patients with stroke or transient ischemic attack: a guideline for healthcare professionals from the American heart association/American stroke association, *Stroke* 42 (2011) pp.227–276.
- [3] J. Fareed, I. Thethi, D. Hoppensteadt, Old versus new oral anticoagulants: focus on pharmacology, *Annu. Rev. Pharmacol. Toxicol.* 52 (2012) pp.79–99.
- [4] A. Maan, R. Padmanabhan, A.Y. Shaikh, M. Mansour, J.N. Ruskin, E.K. Heist, Newer anticoagulants in cardiovascular disease: a systematic review of the literature, *Cardiol. Rev.* 20 (2012) pp.209–221.
- [5] U. Harbrecht, Old and new anticoagulants, *Hamostaseologie* 31 (2011) pp.21–27.
- [6] R.J. Leadley Jr., Coagulation factor Xa inhibition: biological background and rationale, *Curr. Top. Med. Chem.* 1 (2001) pp.151–159.
- [7] T. Xue, S. Ding, B. Guo, Y. Zhou, P. Sun, H. Wang, W. Chu, G. Gong, Y. Wang, X. Chen, Y. Yang, Design, synthesis, and structure-activity and structure-pharmacokinetic relationship studies of novel [6,6,5] tricyclic fused oxazolidinones leading to the discovery of a potent, selective, and orally bioavailable FXa inhibitor, *J. Med. Chem.* 57 (2014) pp.7770–7791.
- [8] U. Trstenjak, J. Ilas, D. Kikelj, Low molecular weight dual inhibitors of factor Xa and fibrinogen binding to GPIIb/IIIa with highly overlapped pharmacophores, *Eur. J. Med. Chem.* 64 (2013) pp.302–313.
- [9] M. Ilic, P. Dunkel, J. Ilas, E. Chabielska, A. Zakrzaska, P. Matyus, D. Kikelj, Towards dual antithrombotic compounds - balancing thrombin inhibitory and fibrinogen GPIIb/IIIa binding inhibitory activities of 2,3-dihydro-1,4-benzodioxine derivatives through regio- and stereoisomerism, *Eur. J. Med. Chem.* 62 (2013) pp.329–340.
- [10] E. Perzborn, S. Roehrig, A. Straub, D. Kubitzka, F. Misselwitz, The discovery and development of rivaroxaban, an oral, direct factor Xa inhibitor, *Nat. Rev. Drug Discov.* 10 (2011) pp.61–75.
- [11] F. Misselwitz, S.D. Berkowitz, E. Perzborn, The discovery and development of rivaroxaban, *Ann. N. Y. Acad. Sci.* 1222 (2011) pp.64–75.
- [12] J.S. Paikin, J.J. Manolagos, J.W. Eikelboom, Rivaroxaban for stroke prevention in atrial fibrillation: a critical review of the ROCKET AF trial, *Expert Rev. Cardiovasc. Ther.* 10 (2012) pp.965–972.
- [13] M.R. Lassen, B.L. Davidson, A. Gallus, G. Pineo, J. Ansell, D. Deitchman, The efficacy and safety of apixaban, an oral, direct factor Xa inhibitor, as thromboprophylaxis in patients following total knee replacement, *J. Thromb. Haemost.* 5 (2007) pp.2368–2375.
- [14] A. De Smedt, M. Cambron, K. Nieboer, M. Moens, R.J. Van Hooff, L. Yperzeele, K. Jochmans, J. De Keyser, R. Brouns, Intravenous thrombolysis with recombinant tissue plasminogen activator in a stroke patient treated with apixaban, *Int. J. Stroke* 9 (2014) pp.E31.
- [15] T. Furugohri, K. Isobe, Y. Honda, C. Kamisato-Matsumoto, N. Sugiyama, T. Nagahara, Y. Morishima, T. Shibano, DU-176b, a potent and orally active factor Xa inhibitor: *in vitro* and *in vivo* pharmacological profiles, *J. Thromb. Haemost.* 6 (2008) pp.1542–1549.
- [16] D.A. Parasrampuria, T. Marbury, N. Matsushima, S. Chen, P.K. Wickremasingha, L. He, V. Dishy, K.S. Brown, Pharmacokinetics, safety, and tolerability of edoxaban in end-stage renal disease subjects undergoing haemodialysis, *Thromb. Haemost.* 113 (2015).
- [17] S.A. Doggrel, Is there evidence to support the use of direct factor Xa inhibitors in coronary artery disease? *Rev. Recent Clin. Trials* 6 (2011) pp.147–157.
- [18] D.J. Pinto, M.J. Orwat, M.L. Quan, Q. Han, R.A. Galemno Jr., E. Amparo, B. Wells, C. Ellis, M.Y. He, R.S. Alexander, K.A. Rossi, A. Smallwood, P.C. Wong, J.M. Luettgen, A.R. Rendina, R.M. Knabb, L. Mersinger, C. Kettner, S. Bai, K. He, R.R. Wexler, P.Y. Lam, 1-[3-Aminobenzisoxazol-5'-yl]-3-trifluoromethyl-6-[2'-(3-(R)-hydroxy-N-pyrrolidin-yl)methyl-[1,1']-biphen-4-yl]-1,4,5,6-tetrahydropyrazolo-[3,4-c]-pyridin-7-one (BMS-740808) a highly potent, selective, efficacious, and orally bioavailable inhibitor of blood coagulation factor Xa, *Bioorg. Med. Chem. Lett.* 16 (2006) pp.4141–4147.
- [19] N.C. Chan, J. Hirsh, J.S. Ginsberg, J.W. Eikelboom, Betrixaban (PRT054021): pharmacology, dose selection and clinical studies, *Future Cardiol.* 10 (2014) pp.43–52.
- [20] P.C. Wong, E.J. Crain, C.A. Watson, A.M. Zaspel, M.R. Wright, P.Y. Lam, D.J. Pinto, R.R. Wexler, R.M. Knabb, Nonpeptide factor Xa inhibitors III: effects of DPC423, an orally-active pyrazole antithrombotic agent, on arterial thrombosis in rabbits, *J. Pharmacol. Exp. Ther.* 303 (2002) pp.993–1000.
- [21] A.C. Gibbs, M.C. Abad, X. Zhang, B.A. Tounge, F.A. Lewandowski, G.T. Struble, W. Sun, Z. Sui, L.C. Kuo, Electron density guided fragment-based lead discovery of ketoheokinase inhibitors, *J. Med. Chem.* 53 (2010) pp.7979–7991.
- [22] A.C. Good, J. Liu, B. Hirth, G. Asmussen, Y. Xiang, H.P. Biemann, K.A. Bishop, T. Fremgen, M. Fitzgerald, T. Gladysheva, A. Jain, K. Jancsics, M. Metz, A. Papoulis, R. Skerlj, J.D. Stepp, R.R. Wei, Implications of promiscuous Pim-1 kinase fragment inhibitor hydrophobic interactions for fragment-based drug design, *J. Med. Chem.* 55 (2012) pp.2641–2648.
- [23] L. Wang, M. Stanley, J.W. Boggs, T.D. Crawford, B.J. Bravo, A.M. Giannetti, S.F. Harris, S.R. Magnuson, J. Nonomiya, S. Schmidt, P. Wu, W. Ye, S.E. Gould, L.J. Murray, C.O. Ndubaku, H. Chen, Fragment-based identification and optimization of a class of potent pyrrolo[2,1-f][1,2,4]triazine MAP4K4 inhibitors, *Bioorg. Med. Chem. Lett.* 24 (2014) pp.4546–4552.
- [24] E.H. Mashalidis, P. Sledz, S. Lang, C. Abell, A three-stage biophysical screening cascade for fragment-based drug discovery, *Nat. Protoc.* 8 (2013) pp.2309–2324.
- [25] L.B. Salum, A.D. Andricopulo, Fragment-based QSAR: perspectives in drug design, *Mol. Divers.* 13 (2009) pp.277–285.

- [26] H. Yuan, T. Lu, T. Ran, H. Liu, S. Lu, W. Tai, Y. Leng, W. Zhang, J. Wang, Y. Chen, Novel strategy for three-dimensional fragment-based lead discovery, *J. Chem. Inf. Model* 51 (2011) pp.959–974.
- [27] M. Sandor, R. Kiss, G.M. Keseru, Virtual fragment docking by glide: a validation study on 190 protein-fragment complexes, *J. Chem. Inf. Model* 50 (2010) 1165–1172.
- [28] H. Liu, T.J. Smith, W.M. Lee, A.G. Mosser, R.R. Rueckert, N.H. Olson, R.H. Cheng, T.S. Baker, Structure determination of an Fab fragment that neutralizes human rhinovirus 14 and analysis of the Fab-virus complex, *J. Mol. Biol.* 240 (1994) pp.127–137.
- [29] K. Yoshikawa, S. Kobayashi, Y. Nakamoto, N. Haginoya, S. Komoriya, T. Yoshino, T. Nagata, A. Mochizuki, K. Watanabe, M. Suzuki, H. Kanno, T. Ohta, Design, synthesis, and SAR of cis-1,2-diaminocyclohexane derivatives as potent factor Xa inhibitors. Part II: exploration of 6-6 fused rings as alternative S1 moieties, *Bioorg. Med. Chem.* 17 (2009) pp.8221–8233.
- [30] J.R. Corte, T. Fang, D.J. Pinto, W. Han, Z. Hu, X.J. Jiang, Y.L. Li, J.F. Gauuan, M. Hadden, D. Orton, A.R. Rendina, J.M. Luettgen, P.C. Wong, K. He, P.E. Morin, C.H. Chang, D.L. Cheney, R.M. Knabb, R.R. Wexler, P.Y. Lam, Structure-activity relationships of anthranilamide-based factor Xa inhibitors containing piperidinone and pyridinone P4 moieties, *Bioorg. Med. Chem. Lett.* 18 (2008) pp.2845–2849.
- [31] L. Anselm, D.W. Banner, J. Benz, K.G. Zbinden, J. Himber, H. Hilpert, W. Huber, B. Kuhn, J.L. Mary, M.B. Otteneder, N. Panday, F. Ricklin, M. Stahl, S. Thomi, W. Haap, Discovery of a factor Xa inhibitor (3R,4R)-1-(2,2-difluoro-ethyl)-pyrrolidine-3,4-dicarboxylic acid 3-[(5-chloro-pyridin-2-yl)-amide] 4-[[2-fluoro-4-(2-oxo-2H-pyridin-1-yl)-phenyl]-amide] as a clinical candidate, *Bioorg. Med. Chem. Lett.* 20 (2010) pp.5313–5319.
- [32] S. Roehrig, A. Straub, J. Pohlmann, T. Lampe, J. Pernerstorfer, K.H. Schlemmer, P. Reinemer, E. Perzborn, Discovery of the novel antithrombotic agent 5-chloro-N-(((5S)-2-oxo-3-[4-(3-oxomorpholin-4-yl)phenyl]-1,3-oxazolidin-5-yl)methyl) thiophene-2-carboxamide (BAY 59-7939): an oral, direct factor Xa inhibitor, *J. Med. Chem.* 48 (2005) pp.5900–5908.
- [33] B. Ye, D.O. Arnaiz, Y.L. Chou, B.D. Griedel, R. Karanjwala, W. Lee, M.M. Morrissey, K.L. Sacchi, S.T. Sakata, K.J. Shaw, S.C. Wu, Z. Zhao, M. Adler, S. Cheeseman, W.P. Dole, J. Ewing, R. Fitch, D. Lentz, A. Liang, D. Light, J. Morser, J. Post, G. Rumennik, B. Subramanyam, M.E. Sullivan, R. Vergona, J. Walters, Y.X. Wang, K.A. White, M. Whitlow, M.J. Kochanny, Thiophene-anthranilamides as highly potent and orally available factor Xa inhibitors, *J. Med. Chem.* 50 (2007) pp.2967–2980.
- [34] D.J. Pinto, M.J. Orwat, S. Koch, K.A. Rossi, R.S. Alexander, A. Smallwood, P.C. Wong, A.R. Rendina, J.M. Luettgen, R.M. Knabb, K. He, B. Xin, R.R. Wexler, P.Y. Lam, Discovery of 1-(4-methoxyphenyl)-7-oxo-6-(4-(2-oxopiperidin-1-yl)phenyl)-4,5,6,7-tetrahydro-1H-pyrazolo[3,4-c]pyridine-3-carboxamide (apixaban, BMS-562247), a highly potent, selective, efficacious, and orally bioavailable inhibitor of blood coagulation factor Xa, *J. Med. Chem.* 50 (2007) pp.5339–5356.
- [35] D. Plewczynski, M. Lazniewski, M. von Grotthuss, L. Rychlewski, K. Ginalski, VoteDock: consensus docking method for prediction of protein-ligand interactions, *J. Comput. Chem.* 32 (2011) pp.568–581.
- [36] D.R. Houston, M.D. Walkinshaw, Consensus docking: improving the reliability of docking in a virtual screening context, *J. Chem. Inf. Model* 53 (2013) pp.384–390.
- [37] J. Xing, Q. Li, S. Zhang, H. Liu, L. Zhao, H. Cheng, Y. Zhang, J. Zhou, H. Zhang, Identification of dipeptidyl peptidase IV inhibitors: virtual screening, synthesis and biological evaluation, *Chem. Biol. Drug Des.* 84 (2014) pp.364–377.
- [38] U. Trstenjak, J. Ilaš, D. Kikelj, Studies towards the synthesis of alkyl N-(4-nitrophenyl)-3/2-oxomorpholine-2/3-carboxylates, *Helvetica Chim. Acta.* 96 (2013) pp.2160–2172.
- [39] P.L.W. Werner, W.K.R. Mederski, Markus Woissyk, Practical and efficient processes for the preparation of 4-(4-aminophenyl)morpholin-3-ones on a larger scale: precursor of factor Xa inhibitors, *Heterocycles* 74 (2007) pp.437–445.
- [40] X.Q. Lewell, D.B. Judd, S.P. Watson, M.M. Hann, RECAP—retrosynthetic combinatorial analysis procedure: a powerful new technique for identifying privileged molecular fragments with useful applications in combinatorial chemistry, *J. Chem. Inf. Comput. Sci.* 38 (1998) pp.511–522.